Article published online: 2021-07-31

Varied appearances & signal characteristics of Leiomyomas on MR Imaging.

BK AGGARWAL, S PANWAR, S RAJAN, A AGGARWAL, K AHLAWAT

Ind J Radiol Imag 2005 15:2:271-276

Keywords: Leiomyomas, MRI

Introduction

Since its inception, the technical quality and range of application of pelvic MRI has steadily increased. MR imaging has emerged as an important imaging modality for evaluation of the female pelvis because of its excellent soft tissue contrast, tissue specificity, lack of ionizing radiation and non-invasive nature [1]. Newer technical innovations of multicoil and fast spin echo sequences have increased the signal to noise ratio & shortened acquisition time. This essay describes the usefulness of MRI in demonstrating location, relationships and characterization of various forms of degeneration in uterine leiomyomas.

Technique:

MR imaging was performed on a 1.5T super-conducting magnet (Symphony, Siemens AG, Erlangen, Germany) using a dedicated phased array body coil. Routine axial T1-weighted, axial, sagittal and coronal T2-weighted images were obtained (Table 1). Additional fat saturated T1-weighted and T2-weighted scans were taken, where necessary

Leiomyomas:

Leiomyomas are the commonest benign uterine tumors occurring in 20-30% of pre-menopausal women [2]. Typical uncomplicated fibroids are well circumscribed, sharply marginated, rounded homogenous masses displaying intermediate signal intensity on T1-weighted images (T1WI), often indistinguishable from the adjacent myometrium. However, optimal contrast is achieved on T2-weighted images (T2WI), where they are hypointense relative to the myometrium [3, 4]. The typical MR imaging feature of leiomyoma-distinct low signal intensity on T2-weighted images-is due to extensive hyalinization [5,6].

Ninety percent of these are located in the corpus uteri in the Intramural (when bulk of the tumor was within the myometrium) (Fig 1), subserosal (when the epicenter of the lesion is beyond the outer uterine wall), or submucosal (when they protrude into the endometrial cavity) locations (Fig 2) [2]. Five percent each are located in the cervical (Fig 3) & broad ligament regions respectively (Fig 4,5). Prolapse (Fig 6) and partial detachment of the myomas have also been seen.

Table 1: Sequences used for Routine MR examination of the Pelvis

	Axial TSE T2	Axial T1	Coronal TSE T2	Sagittal TSE T2	Axial TSE T2 FS	Axial T1 FS
TR (msec)	5300	550	4200	4850	4380	400
TE (msec)	96	14	105	105	99	13
Flip Angle(deg)	150	90	150	150	150	90
Number of Excitations	2	2	1 *	2	3	2 #
Matrix	256x256	256x256	512x307	512x282	256x256	256x256
Slice thickness	8mm	8mm	4-5 mm	4-5 mm	4mm	4mm
Turbo Factor	17	-	13	15	17	-
Saturation band				Sagittal over anterior abdominal wall	Fat saturation	Fat Saturation

• * Oversampling of 100%
• # Concatenation factor of 2

From the Diwanchand Aggarwal Imaging & Research Centre, 10-B K.G. Marg, New Delhi - 110001

Request for Reprints: Dr Bharat K Aggarwal, 10-B Kasturba Gandhi Marg, New Delhi – 110 001

Received 10 June 2003; Accepted 15 December 2004

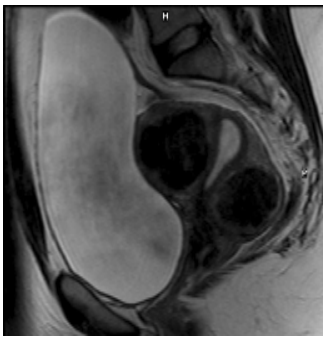

Figure 1 34-year-old woman with multiple anterior and posterior wall leiomyomas.

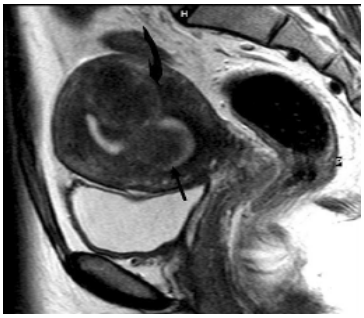

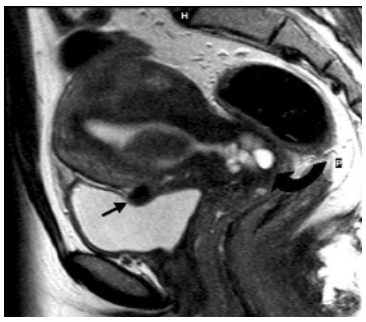

Figure 2 30-year-old woman with multiple leiomyomas.
A Parasagittal T2weighted image shows a submucosal fibroid (arrow) arising from the anterior wall and a intramural fibroid arising from the posterior wall (curved arrow). The latter has its epicenter within the myometrium.
B Sagittal T2 weighted image from the same study shows a small subserosal fibroid (arrow). Multiple hyperintense Nabothian cysts are also seen (curved arrow).

Figure 3 40-year-old woman with a cervical fibroid.
A Midline sagittal T2 weighted scan.
B Para-sagittal scan from the same series.

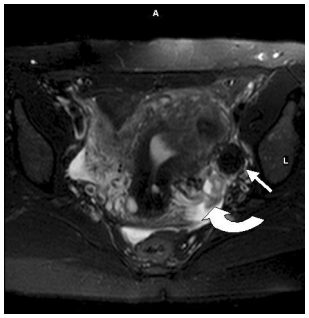

Figure 4 41-year-old woman with a broad ligament fibroid. Axial fat saturated T2 weighted scan shows the fibroid as a well-defined hypointense mass in the left adnexa (arrow). The left ovary is seen separately, posterior to the fibroid (curved arrow).

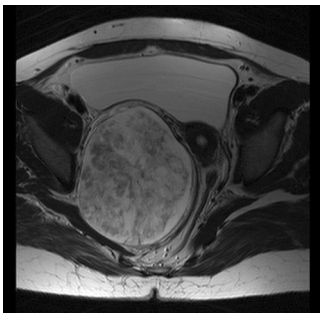

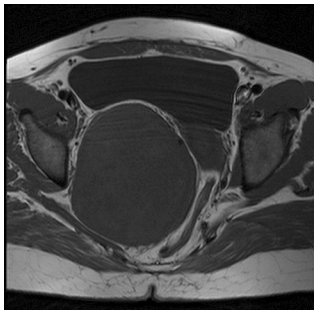

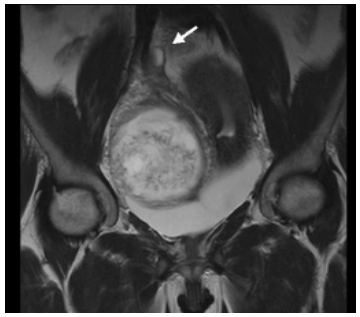

Figure 5 36-year-old woman with a degenerated broad ligament fibroid.
A Axial T2 weighted scan shows a large hyperintense right adnexal mass showing whorl like internal low signal areas. The increased T2 hyperintensity was due to associated myxoid degeneration.
B Axial T1 weighted scan at the same level shows the mass to be isointense with the whorl-like areas barely perceptible
C Coronal T2 weighted scan showing the right ovary (arrow) identified separate from this mass and the uterus.

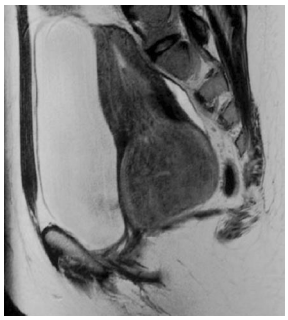

Figure 6 19-year-old girl with a prolapsed submucosal fibroid. Sagittal T2 weighted scan shows the hypointense mass prolapsing from the uterine corpus into the cervix. The pedicle is also seen.

Figure 7 23-year-old woman with a leiomyoma showing hyaline degeneration. Sagittal T2 weighted scan showing a large well marginated fibroid showing "speckled" signal intensities.

Figure 8 40-year-old woman with cystic degeneration in a leiomyoma.
A Sagittal T2 weighted scan showing a fluid-fluid level in a well marginated anterior myometrial mass showing characteristic low signal intensity wall.
B Another image from the same series showing the normal endometrium (arrow) lying posterior to this mass. A hydro/pyometra can occasionally be confused with cystic degeneration.

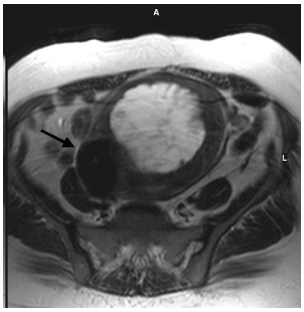

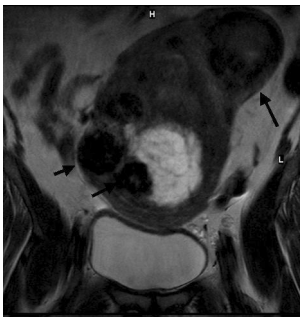

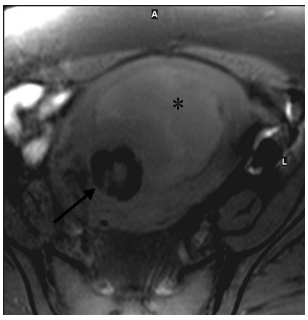

Figure 9 48-year-old woman with multiple fibroids showing hemorrhagic / red degeneration and calcifications.
A Sagittal T2 weighted image shows a heterogeneous hyperintense mass with a hypointense rim in the anterior myometrium.
B Axial T2 weighted image shows additional hypointense leiomyoma in the right lateral myometrium (arrow).
C Coronal T2 weighted image shows multiple additional leiomyomas(arrows).
D Axial T1 weighted fat saturated image shows the hyperintense mass in A also showing increased signal intensities, indicating hemorrhagic component. The leiomyoma in the right lateral myometrium shows a thick hypointense rim indicating rim calcification.
E Plain radiograph of the abdomen, showing the rim calcification in some of these myomas.

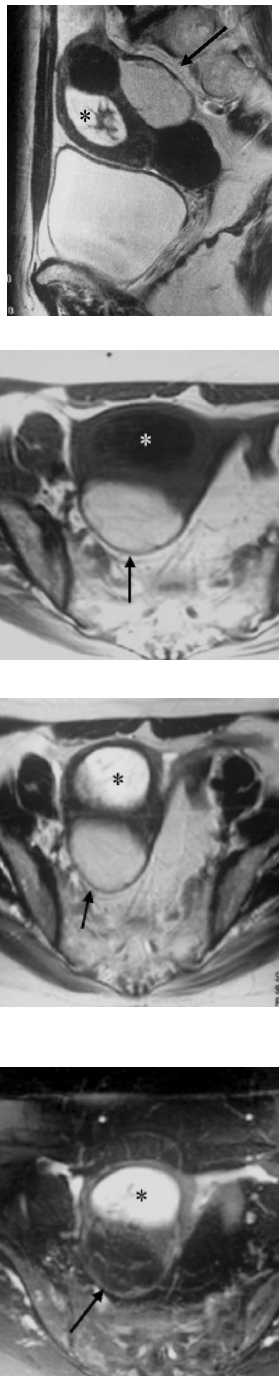

Figure 10 45-year-old woman on tamoxifen for previously treated breast carcinoma with endometrial hyperplasia and multiple leiomyomas, one being a lipoleiomyoma.
A Sagittal T2 weighted scan showing endometrial hyperplasia (asterix) with low signal intensity leiomyomas in the fundus and lower segments. The leiomyoma in the mid posterior myometrium is hyperintense on this sequence.
B The leiomyoma continues to be hyperintense on the T1 weighted axial image (arrow) and the endometrium (asterix) displayes low signal intensity.
C Axial T2 weighted image shows increased signal within the leiomyoma (arrow) as well as the endometrium.
D Axial fat-saturated image shows signal drop-off in the leiomyoma (arrow) indicating presence of fat. The endometrium continues to show increased signals.

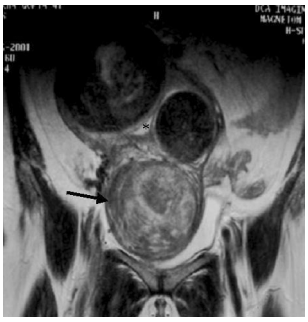

Figure 11 44-year-old woman with multiple intra-mural leiomyomas indenting the endometrial cavity (asterix). One of the leiomyomas (arrow) is degenerated, displaying increased signal intensity on this coronal T2 weighted scan.

Figure 12 37-year-old woman with adenomyosis and a leiomyoma.
A Sagittal T2 weighted scan showing an area of poorly marginated hypointensity in the posterior myometrium inseparable from the junctional zone, suggestive of a focal area of adenomyosis (adenomyoma).
B Coronal T2 weighted image showing the same area. The left ovary shows altered signal intensities with areas of high and low signal, indicating hemorrhagic contents.
C Axial fat saturated T2 weighted scan in the same patient showing a well marginated, rounded low signal intensity anterior wall intra-mural leiomyoma.

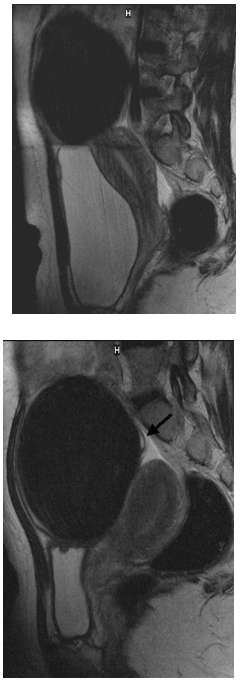

Figure 13 27-year-old woman with a right ovarian fibroma. (Reprinted with permission from [8])
A Sagittal T2 weighted scan shows a well defined hypointense mass located antero-superior to the uterine fundus.
B A post-void sagittal T2 weighted scan in the same woman shows change in position of this lesion, which now lies anterior to the uterus. A small cystic follicle is seen in relation to the lesion (arrow). The right ovary was not identified separately.

Degenerative Leiomyomas

To understand the wide spectrum of MR imaging findings, unusual appearances of leiomyomas can be classified into three categories: degeneration and other histopathologic findings, specific types of unusual leiomyomas, and unusual growth patterns.

The common types of degeneration are hyaline (>60% of cases) [6], cystic (~4%), myxoid, and red. Edema is not a phenomenon of degeneration but is a common histopathologic finding (~50% of cases). Hemorrhage, necrosis, and calcification (~4% of cases) may also be observed. Specific types of unusual leiomyomas include lipoleiomyoma and myxoid leiomyoma, which may have MR imaging features characteristic enough to allow differentiation from other gynecologic and nongynecologic diseases. Intravenous leiomyomatosis, metastasizing leiomyoma, diffuse leiomyomatosis, and peritoneal disseminated leiomyomatosis represent unusual growth patterns; other unusual growth patterns are retroperitoneal growth & parasitic growth [5].

A variety of degenerations alter the signal intensity of leiomyomas that demonstrate a characteristic speckled or heterogeneous pattern, exhibiting areas of high signal intensity interlacing within low intensity masses [3]. The alteration in signal intensity on T2WI depends on the degree of cellularity, hyalinization & hemorrhage [4, 7]. Hyaline degeneration is the commonest form producing a characteristic "speckled" pattern (Fig 7).

Edema may change into various degrees of collagen deposition and cystic degeneration. Cystic degeneration may be considered an extreme sequel of edema and is observed in about 4% of leiomyomas. Large or small cystic spaces develop in the edematous, acellular center. The cystic spaces appear as round, well-demarcated areas with the signal intensity characteristic of fluid: low on T1-weighted images and high on T2-weighted images with no enhancement (Fig 8). Myxoid material demonstrates high signal intensity on the T2-weighted image, low signal intensity on the T1-weighted image. Viable tissue has relatively low signal intensity on the T2-weighted image [5]

Red or carneous degeneration involves massive hemorrhagic infarction of a leiomyoma due to obstruction of drainage veins at the periphery of the lesion. Such degeneration is a kind of extensive coagulative necrosis that involves the entire lesion. This condition occurs most often during pregnancy [3], and is also associated with use of oral contraceptives. Unlike other types of degeneration, red degeneration usually causes systemic symptoms. Findings at MR imaging reflect the pathogenesis of this condition well and contribute to an accurate diagnosis. The peripheral rim, which has distinct low signal intensity on T2-weighted images and high signal intensity on T1-weighted images, corresponds to the obstructed veins at the periphery of the mass [5]. Hemorrhage in a myoma may have variable MR appearances depending on imaging sequence used & stage of evolution of the bleed [4] (Fig 9).

Although calcification has no specific MR appearance, lack of signal within masses that does not change with different TR & TE parameters is highly suggestive of calcification [2]. We have found this most apparent on fat saturated T1 weighted scans. The calcification is usually dense and amorphous. This pattern of calcification at plain radiography almost exclusively indicates the diagnosis of leiomyoma. A rarely observed pattern is ringlike calcification at the margins of a leiomyoma (Fig 9). This type of calcification appears to represent thrombosed veins from past red degeneration [5].

Lipoleiomyoma / fatty degeneration is easy to diagnose, being hyperintense on T1WI with a characteristic signal drop-off on fat suppressed sequence (Fig 10). Larger myomas having speckled & whorled appearance containing interspersed mucinous & myxomatous material are often difficult to specifically distinguish on MR (figure

11), as is the rare sarcomatous change [2, 3, 4]. Hemorrhage and necrosis (other than red degeneration) are not common but may be observed in leiomyomas.

Differential Diagnosis:

Leiomyomas & adenomyosis having the same clinical presentation & frequent concurrent occurrence often pose pre-op diagnostic dilemmas, especially focal adenomyosis (Adenomyoma). The former is amenable to conservative (myomectomy) & the latter to radical surgery (hysterectomy). MR imaging is sensitive in reflecting the pathological difference between the two [1,3]. The less vascularity with lack of edema & the ectopic migration of the endometrium into the myometrium causing the adenomyotic foci to inter-digitate are responsible for its low signal, ill-defined margins & contiguity with the junctional zone. Myomas, in turn, are well defined due to the halo of compressed adjacent myometrium forming a pseudo-capsule (Fig 12). Also leiomyomas are round in comparison to adenomyomas which tend to be oval along the long axis of the uterus [1, 3].

Often it is impossible to distinguish a solid adnexal tumor lying in close proximity to the uterus from a pedunculated subserosal fibroid on sonography alone, especially if both the ovaries are not identified. One such example being ovarian fibroma which displays similar signal intensity as myoma on MR [8]. Non-visualisation of the ovary or visualization of a remnant follicle at its periphery, and change in position of the mass in relation to the uterus on pre-post void imaging gives the diagnosis (Fig 13).

Leiomyomas are often associated with numerous obstetric complications including decreased fertility, the mechanism of which is not known. Myomectomy has resulted in improved fertility in some of the cases. Although ultrasound is the initial screening modality, sonographic limitations include marked uterine distortion, multiplicity of lesions, operator dependence & tumor size. MR outperforms ultrasound & hysterosalpingograms in the same [9].

Contrast enhanced T1WI do not improve the assessment of fibroids except when in unusual location or when unenhanced T2WI are of inferior quality [10]. They may also have a role in pre-embolisation evaluation to control excessive menorrhagia.

Conclusion:

MRI is an accurate means available for precise determination of location, relationships and detection of degeneration within these benign tumors of the uterus. The precise type of degeneration can also often be characterized by MR, providing pertinent information before any surgical intervention is contemplated.

References:

1. Mark AS, Hricak H : Adenomyosis & leiomyomas : Differential diagnosis by means of MRI. Radiology 163: 527,1987.
2. Hricak H, Tscholakoff D, Heinrichs L, et al : Uterine leiomyomas correlation by Magnetic Resonance Imaging : clinical symptoms & histopathology. Radiology 158: 385, 1986.
3. Togashi K, Ozaka H, Konishi I, et al : Enlarged uterus : Differentiation between adenomyosis & leiomyomas with MRI. Radiology 171: 531,1989.
4. Hamlin DJ, Pettersson H, Fitzsimmons J, et al : MR imaging of uterine Leiomyomas & their complications. J Comput Assist Tomography 9:902, 1985.
5. Ueda H, Togashi K, Konishi I , et al. Unusual Appearances of Uterine Leiomyomas: MR Imaging Findings and Their Histopathologic Backgrounds Radiographics. 1999;19:S131-S145.
6. Rosai J. Ackerman's surgical pathology 8th ed. St Louis, Mo: Mosby-Year Book, 1996; 1429-1433.
7. Weinreb JC, Barkoff ND, Megibow A, et al : The value of MR imaging in distinguishing leiomyomas from other solid pelvic masses when sonography is indeterminate. Am J of Roentgenology 154: 295, 1990.
8. Chopra S, Ahlawat K, Aggarwal B, et al: Demonstration of an Ovarian Fibroma by ultrasound and MRI: A Case Report. Asian Oceanian Journal of Radiology. Vol. 7 No 2; 84-87, 2002.
9. Dudiak CM, Turner DA, Patal SK, et al : Uterine leiomyomas in the infertile patient : Pre-operative localization with MRI versus US & HSG. Radiology 167: 627, 1988.
10. Hricak H, Finck S, Honda G, et al : MR imaging in the evaluation of benign uterine masses : value of gadopentetate dimeglumine enhanced T1W images. Am J of Roentgenology 158: 1043, 1992.